Geodesy and Geodynamics xxx (xxxx) xxx

Contents lists available at ScienceDirect

Geodesy and Geodynamics

journal homepage: http://www.keaipublishing.com/geog

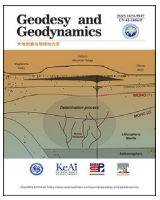

Research Paper

Spatiotemporal evolution of long-term slow slip events at the Hikurangi subduction zone, New Zealand (2021–2023): Implications for seismic activity

Li Yan [a, b, c, d, *], Yanling Sun [a, c, d], Meng Li [a, b, c, d], Ahmed El-Mowafy [b], Tieding Lu [a, c, d]

[a] Jiangxi Key Laboratory of Watershed Ecological Process and Information (Platform No. 2023SSY01051), East China University of Technology, Nanchang, 330013, China
[b] School of Earth and Planetary Sciences (Spatial Sciences), Curtin University, GPO Box U1987, Perth, WA 6845, Australia
[c] Key Laboratory of Mine Environmental Monitoring and Improving Around Poyang Lake of Ministry of Natural Resources, East China University of Technology, Nanchang, 330013, China
[d] Nanchang Key Laboratory of Landscape Process and Territorial Spatial Ecological Restoration, East China University of Technology, Nanchang, 330013, China

ARTICLE INFO

Article history:
Received 9 September 2024
Received in revised form
11 November 2024
Accepted 5 December 2024
Available online xxx

Keywords:
Long-term slow slip events
Spatiotemporal evolution
Seismic activity
GNSS
New Zealand

ABSTRACT

Various slow slip events (SSEs) with distinct characteristics have been detected globally, particularly in regions with dense Global Navigation Satellite Systems (GNSS) networks. In the Hikurangi subduction zone of New Zealand, SSEs frequently occur alongside seismic activity, especially in the Manawatu and Kapiti regions. This study analyzes the 2021–2023 Kapiti-Manawatu long-term SSE using daily displacement data (2019–2023) from 53 GPS stations. The network inversion filter (NIF) method is applied to extract slow slip signals, revealing spatial migration with alternating slip between Kapiti and Manawatu, characterized by distinct phases of acceleration and deceleration. Manawatu exhibits higher slip rates, exceeding 4 cm/month, with greater cumulative slip and surface displacement than Kapiti. A moderate temporal correlation (coefficient 0.59) between seismic activity in the region and slip acceleration in Manawatu suggests that seismic events may contribute to the slip, while no significant correlation is observed in Kapiti.

1. Introduction

Slow slip events (SSEs) are transient slip phenomena occurring around fault zones, typically found in the transitional regions between the locked and stable creeping zones of subduction zones [1]. These events help release the stress accumulated in tectonic plates due to tectonic movements. Unlike earthquakes, which last only a few seconds, the strain between plates during slow slips is released over several days to years, producing minimal seismic waves [1]. Detecting slow slip requires high-density observations of crustal deformation. Dense Global Navigation Satellite Systems (GNSS) networks in subduction zone regions can used to detect millimeter-scale surface movements, accurately recording transient deformation signals, including slow slip [2,3]. This provides valuable and precise data for earthquake research in subduction zones. Various SSEs with different characteristics have been detected in multiple subduction zones worldwide [4], primarily in regions such as Japan [5–7], Cascadia [8,9], Mexico [10–12], and New Zealand [13–15], as shown in Fig. 1.

The Hikurangi subduction zone in New Zealand (Fig. 2) results from the westward subduction of the Pacific Plate beneath the North Island [16]. Beneath the eastern coast, the subduction interface is relatively shallow, with SSEs recorded at depths of 15–20 km [17]. As the interface depth increases westward, the coverage depth range expands, benefitting land-based geodetic studies. Research indicates that there are two types of SSEs: short-term and long-term [18–20]. These events can cause displacements

* Corresponding author. Jiangxi Key Laboratory of Watershed Ecological Process and Information (Platform No. 2023SSY01051), East China University of Technology, Nanchang, 330013, China.
E-mail address: yanli20060675@foxmail.com (L. Yan).

Peer review under the responsibility of Institute of Seismology, China Earthquake Administration.

https://doi.org/10.1016/j.geog.2024.12.001

Please cite this article as: L. Yan, Y. Sun, M. Li *et al.*, Spatiotemporal evolution of long-term slow slip events at the Hikurangi subduction zone, New Zealand (2021–2023): Implications for seismic activity, Geodesy and Geodynamics, https://doi.org/10.1016/j.geog.2024.12.001

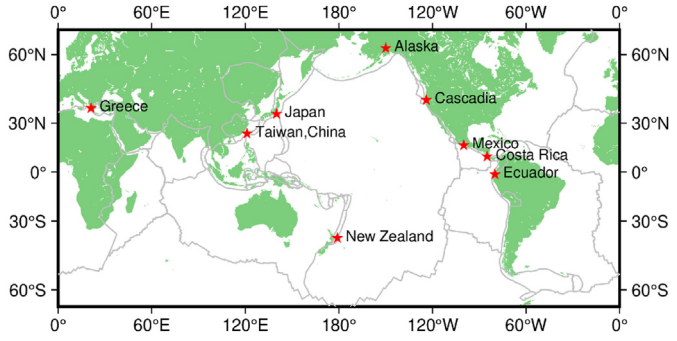

Fig. 1. Global distribution of major global SSEs. The thick gray solid lines indicate the global tectonic plate boundaries, and the red pentagrams represent the locations of SSEs in subduction zones.

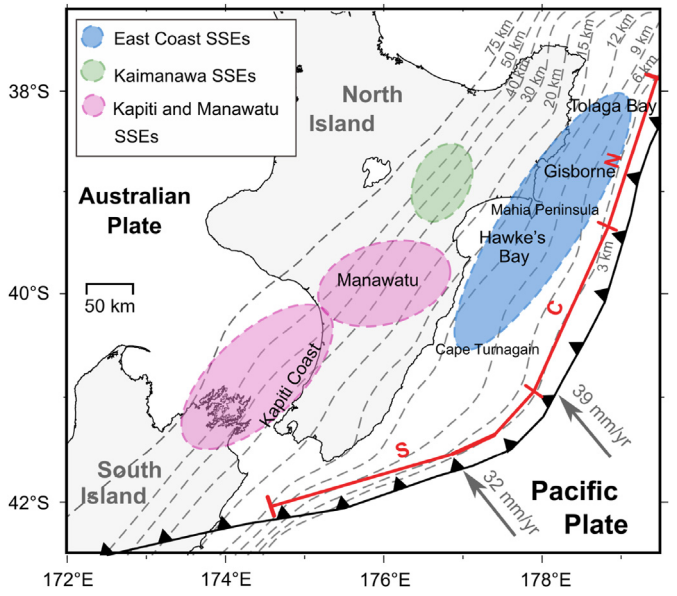

Fig. 2. Tectonic background and historical SSEs in the Hikurangi subduction zone, New Zealand. The light blue shaded areas indicate short-term slow slip regions along the east coast of the North Island [22,28,30–32]. The light green area represents the Kaimanawa short-term slow slip region [23]. The magenta shaded area indicates the Kapiti-Manawatu long-term slow slip region [24,26–28,32–35]. The thick red solid line divides the Hikurangi subduction zone into northern, central, and southern segments, labeled as N, C, and S, respectively. Gray dashed lines represent the depth contours of the plate interface. The gray arrows show the normal convergence rate of the Hikurangi trench towards the Australian Plate.

from a few to several tens of centimeters on the plate interface, with equivalent moment magnitudes of about M_W7.0. Short-term SSEs [13,21,22], lasting no more than 3 months and recurring every 1–2 years, are primarily found along the eastern coast of New Zealand's North Island and in the central Kaimanawa region [23]. On the eastern coast, these events occur at shallow depths (<20 km), whereas in the Kaimanawa region, they happen at depths of 30–40 km, about 75 km from Hawke's Bay. Long-term SSEs last 12–18 months, occurring every 5 years, and typically happen in the Manawatu and Kapiti regions of the southern part of the North Island at depths of 30–50 km [24–28]. This contrasts with other subduction zones, like Cascadia and Nankai in Japan, where long-term SSEs occur at shallow depths (15–30 km), and short-term SSEs are found deeper (30–45 km) [29].

The Hikurangi subduction zone exhibits frequent seismic activity, with significant differences in the spatiotemporal evolution characteristics of long-term and short-term SSEs [18]. The relationships among these events remain to be fully understood. Previous studies have indicated that long-term SSEs can alter the stress state of the seismogenic zone, affecting the recurrence intervals of short-term SSEs [5,26,29] and promoting earthquake nucleation [12,36]. Wallace et al. inverted SSEs on the Hikurangi subduction zone during 2010–2011 [26], finding that long-term SSEs in the Manawatu region of the North Island begin a year before the short-term SSEs on the east coast. By calculating Coulomb stress changes, they suggested that long-term SSEs might have triggered subsequent short-term SSEs. Radiguet et al. discovered a long-term SSE lasting approximately 10 months in their analysis of the April 2014, M_W7.3 earthquake in Mexico [12]. This SSE migrate along the fault toward the earthquake rupture zone in the two months preceding the earthquake, leading them to propose that the M_W7.3 Papanoa earthquake is triggered by the long-term SSE. Therefore, studying long-term SSEs can provide insights into the stress state of locked plate boundary zones and help assess the likelihood of subduction zone earthquakes.

This study uses daily displacement data from 53 GNSS stations in central and southern North Island, New Zealand, obtained through GOENET, to extract time series with long-term slow slip signals from 2021 to 2023. We applied the Network Inversion Filter (NIF) method based on the Kalman filter [37] to invert the spatiotemporal evolution of long-term SSEs in the Kapiti and Manawatu regions of the Hikurangi subduction zone. The NIF method effectively uses GNSS networks to invert the spatiotemporal slip distribution of subsurface faults [38,39] and has been successfully applied to study various SSEs [21,29,40,41]. We also examine the spatial and temporal relationship between long-term SSEs and seismic activity to reveal the connection between these events and regional seismic activity in the Hikurangi subduction zone.

2. Data and methodology

The monitoring data for long-term SSEs in the Hikurangi subduction zone from 2021 to 2023 are obtained from the GNSS network deployed by GeoNet in New Zealand. This study primarily utilizes surface displacement coordinate time series from 53 GNSS stations located in central and southern North Island, as shown in Fig. 3. The GNSS network has been operational since 2002 and uses the GAMIT/GLOBK software developed and maintained by the Department of Earth, Atmospheric, and Planetary Sciences at MIT (https://www.geonet.org.nz/data/types/geodetic). It resolves coordinates in the ITRF2008 reference frame for the east (E), north (N), and up (U) directions, with horizontal and vertical accuracies within 3 mm and 7 mm, respectively. This network is primarily used for monitoring and analyzing crustal activities such as earthquakes, landslides, tsunamis, and volcanic events in New Zealand.

In Fig. 3, the Pacific plate subducts westward beneath the North Island of New Zealand along the Hikurangi trench, with a normal convergence rate of approximately 32 mm/year [42]. The Hikurangi subduction zone exhibits significant north-south variations in its tectonic characteristics and can be divided into three main segments: northern, central, and southern. Short-term shallow SSEs are typically detected near the coast in the northern and central segments. In contrast, this study focuses on long-term deep SSEs occurring mainly in the southern Kapiti coast and central Manawatu region, within the transition zone between the shallow locked zone and the deeper stable sliding zone.

Using the surface displacement coordinate time series of these GNSS stations shown in Fig. 3, the modeling and inversion of long-

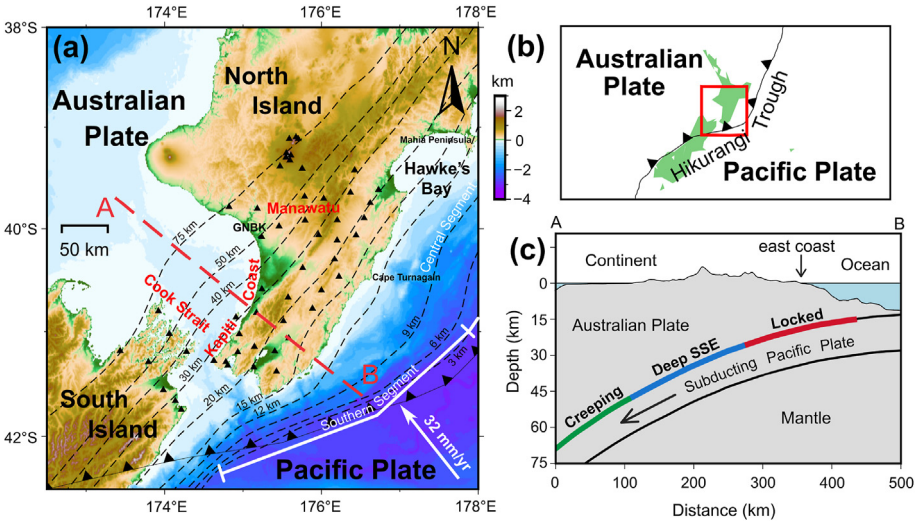

Fig. 3. (a) Geological structure of the Hikurangi subduction zone, New Zealand. The black solid triangles represent 53 GNSS stations distributed across the southern North Island and northern South Island of New Zealand, and the black dashed lines are depth contour lines of the plate interface [43]. The thick white solid lines segment the Hikurangi subduction zone along the trench, indicating the southern segment of the subduction zone. The white arrows show the normal convergence rate of the Hikurangi trough towards the Australian Plate. (b) indicates the study area shown in (a) with a red rectangle, where the Hikurangi subduction zone is located at the convergent margin of the Pacific and Australian Plates. (c) shows the cross-section along the red dashed line A-B in (a), illustrating the position of deep slow slip on the subduction plate interface.

period slow slip signals can be described by the following equations [37,44,45]:

$$X(t) = X_0(t_0) + vt + \sum_j b_j H(t - t_j) + \sum_i [S_i \sin(\varpi_i t) + C_i \cos(\varpi_i t)] + X_{SSE}(x,t)$$
$$X_{SSE}(x,t) = \int_A G(x,\xi) S(\xi,t) dA(\xi) + F(x) f(t) + B(x,t) + \varepsilon(x,t) \quad (1)$$

where, $X(t)$ is the GNSS coordinate series at time t; $X_0(t_0)$ is the initial position of GNSS station at the starting time t_0; v is the long-term steady-state velocity; $H(t-t_j)$ is the Heaviside step function, and b_j is the step amplitude at time t_j; S_i and C_i represent the amplitudes of seasonal periodic variations, and ϖ denotes the phase; $X_{SSE}(x,t)$ is the displacement time series containing the slow slip signal. In the NIF method, $X_{SSE}(x,t)$ is decomposed into four components: surface deformation $\int_A G(x,\xi) S(\xi,t) dA(\xi)$ caused by the slow slip, common-mode error $F(x)f(t)$, reference oscillation $B(x,t)$, and random noise $\varepsilon(x,t)$. Here, $S(\xi,t)$ represents the slip at location ξ on fault plane A at time t. The Green's function $G(x,\xi)$ relates the slip at location ξ on the fault to the displacement at surface location x.

Taking the GNBK station (as shown in Fig. 3) as an example, the modeling to obtain long-term slow slip signals is illustrated in Fig. 4. Using the GNSS coordinate time series spanning from January 1, 2019, to December 31, 2023, we extracted long-term slow slip signals after 2021. The steps are as follows: First, remove gross errors from the GNSS coordinate time series, using the three-sigma of the residuals as a threshold for detection of outliers in the observations, and correct for step discontinuities (Fig. 4(a)). Then, estimate the steady-state tectonic motion and seasonal periodic term coefficients using the GNSS coordinate time series from January 1, 2019, to December 31, 2020, when no slow slip occurred. Finally, remove the steady-state tectonic motion (Fig. 4(b)) and seasonal periodic variations (Fig. 4(c)) from the entire time series to obtain the long-term slow slip displacement time series (Fig. 4(d)). The period from January 2019 to December 2020, during which no SSEs occur, is selected to estimate the tectonic motion rate and seasonal periodic term coefficients. This choice is based on prior research indicating that alternating SSEs in the Kapiti and Manawatu regions from 2003 to 2018 [24,25,27,28,33]. When studying long-term tectonic motion, it is essential to exclude periods with SSEs to obtain a reliable long-term velocity estimate [32]. Additionally, earthquakes can cause corresponding changes in GNSS displacement data in both horizontal and vertical directions [46] especially moderate-to-strong events. Within the study area and timeframe, no earthquake events caused significant GNSS surface displacement changes, so the influence of seismic events is not considered in the GNSS data processing for this study.

To invert the corresponding fault slip from the long-term slow slip displacement time series, a 3D fault grid model must be constructed, as shown in Fig. 5. The 3D fault grid model of the Hikurangi subduction zone, corresponding to the long-term slow slip in the Kapiti-Manawatu Region, was obtained by interpolating isodepth contours [43]. The depth ranges from 6 to 75 km and includes 3437 triangular grid cells, with the shortest edge length of 10 km. Referencing fault model parameters used in previous studies of the Hikurangi subduction zone [24,27,31,32,47], the shortest grid size for the Hikurangi subduction interface model can be set between 3 and 20 km [27,32,47]. In Ref. [24], a grid size of 6×3 km^2 quadrilaterals is used, while Ref. [31] employed a 3D irregular grid with a resolution of 25×20 km^2. In this

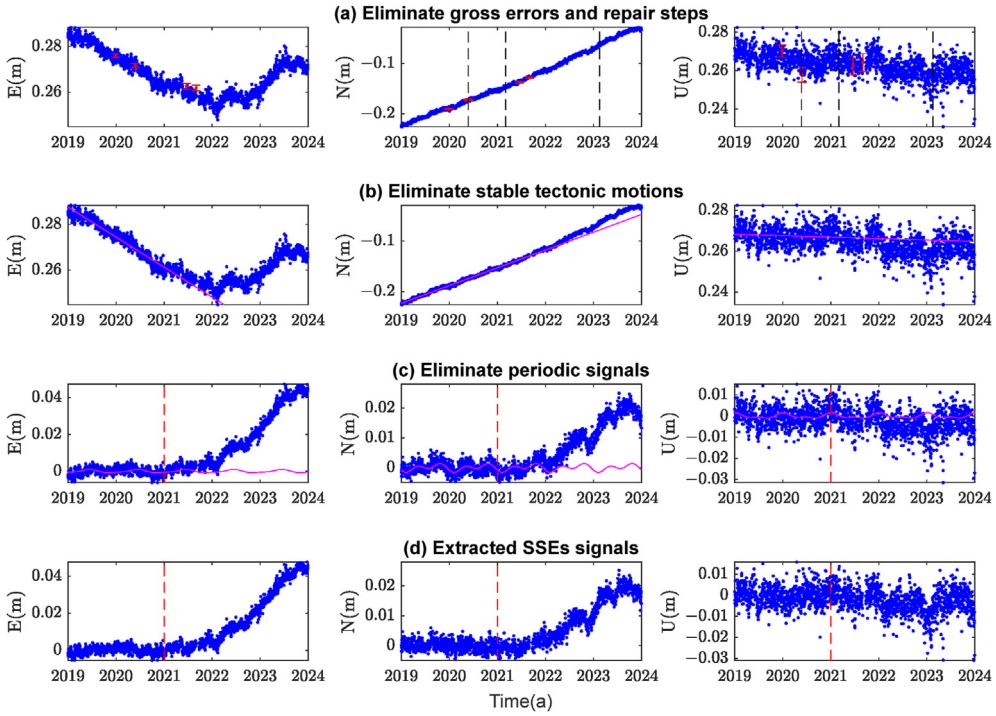

Fig. 4. Extraction process of GNSS slow slip signals (example from station GNBK).

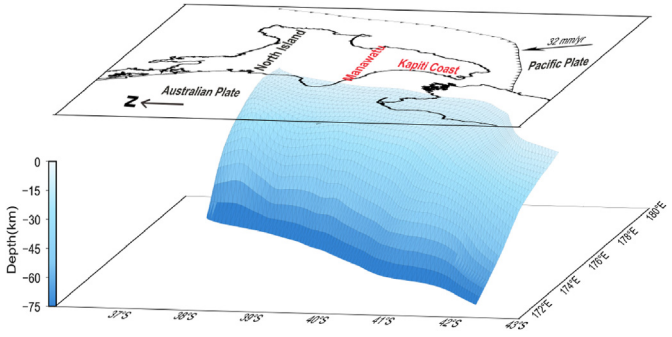

Fig. 5. Fault geometry model of the Hikurangi subduction zone.

study, we test a fault grid with a minimum size of 10 km, achieving a satisfactory balance between model smoothness and slip uncertainty. Based on this 3D fault grid model, the fault Green's function is calculated, and the noise model is set to a random walk model. The NIF method is used for filtering to obtain the fault slip.

3. Results

3.1. Monthly slip rate of Kapiti-Manawatu long-term SSE (2021–2023)

Fig. 6 illustrates the spatiotemporal evolution of the long-term SSE in the Kapiti-Manawatu region from 2021 to 2023. The figure reveals a spatial migration process of the long-term slow slip between the Kapiti and Manawatu areas, as well as intermittent stages of acceleration and deceleration in the slip. Accordingly, three stages can be approximately delineated: Stage 1 (May 2021 to July 2022), Stage 2 (August 2022 to August 2023), and Stage 3 (September 2023 to December 2023). In Stage 1, the slip in the Kapiti region accelerates, reaching a maximum of 2.03 cm/month (September 2021), followed by a deceleration phase during which the slip migrates toward the Manawatu region, where the maximum monthly slip rate reaches 4.26 cm/month (March 2022) before decelerating. Stage 2 shows a gradual acceleration of slip in the Kapiti region, reaching a maximum of 3.43 cm/month (January 2023). During the deceleration phase, the slip migrates toward the Manawatu region, with the maximum monthly slip rate reaching 4.01 cm/month (May 2023) before decelerating. During the first two stages, the slip in the two regions exhibits an inverse relationship, while in Stage 3, the slip in both regions tends to accelerate simultaneously, with slip rates reaching 2.01 cm/month and 4.4 cm/month, respectively, with no subsequent deceleration observed. This suggests that the long-term SSE in the Kapiti-Manawatu region is likely to continue in 2024.

During the acceleration stages of the long-term SSE from 2021 to 2023, the Manawatu region experiences three instances of acceleration, each with a maximum monthly slip rate exceeding 4 cm/month, while the Kapiti region experiences three instances of acceleration with maximum monthly slip rates ranging between 2 and 3.5 cm/month. This indicates that the maximum monthly slip rate in the Manawatu region exceeds that in the Kapiti region throughout the long-term SSE.

3.2. Three stages of Kapiti-Manawatu long-term SSE

Fig. 7 presents the cumulative slip and surface displacement during the aforementioned three stages. In Fig. 7, the maximum cumulative slips in the Kapiti/Manawatu regions during the three stages are 4.47/8.94, 13.21/11.55, and 3.77/5.51 cm, respectively, with the maximum surface displacements monitored by GNSS are 1.77, 3.31, and 0.73 cm, respectively. Additionally, the cumulative slip uncertainty across the three stages does not exceed 3.2 mm (Fig. S1). The surface displacement derived from the NIF method and that monitored by GNSS show minor discrepancies due to the influence of common-mode errors, reference oscillation, and random noise, but they are generally in agreement.

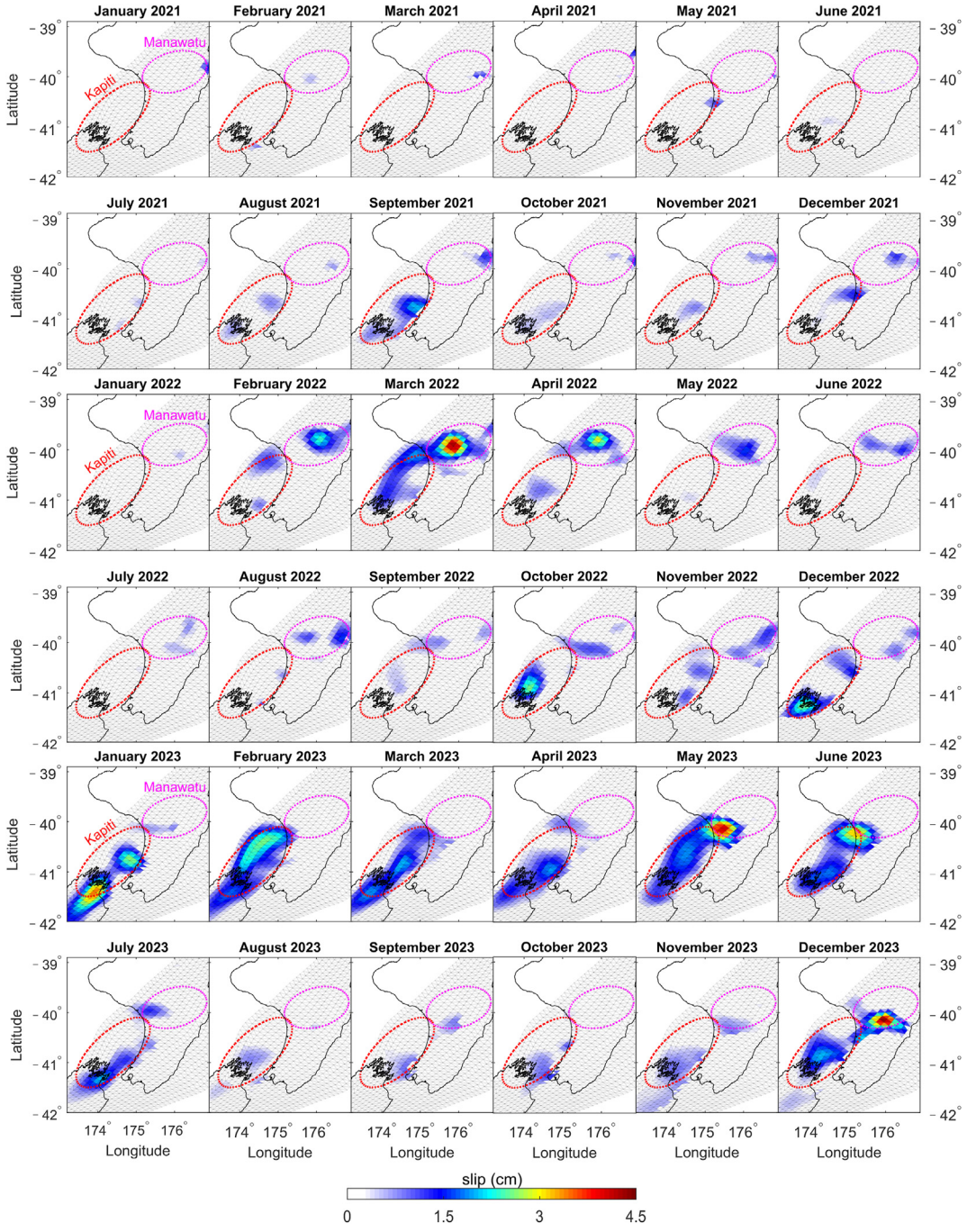

Fig. 6. Monthly slip rate of Kapiti-Manawatu long-term SSE (2021–2023).

The timing, maximum monthly slip rate, cumulative slip, and surface displacement during the three stages of the Kapiti-Manawatu long-term SSE from 2021 to 2023 are summarized in Table 1. Stage 1 and Stage 2 represent two complete cycles of spatial migration and acceleration-deceleration, each lasting approximately one year. The cumulative slip and surface displacement in the Kapiti-Manawatu region during Stage 2 are greater than those in Stage 1.

3.3. Correlation between long-term SSEs and seismic activity

To further analyze the relationship between the Kapiti-Manawatu long-term SSE (2021–2023) and seismic activity, a statistical examination of the New Zealand earthquake catalog (https://quakesearch.geonet.org.nz/ (accessed on March 1, 2024)) is conducted. Seismic events occurring within the Kapiti-Manawatu region (KMR) at a depth range of 0–80 km are selected for a correlation analysis with the long-term SSE slip rates, as shown in Fig. 8 and Table 2.

In Fig. 8, during the two complete cycles of spatial migration and acceleration-deceleration (Stage 1 and Stage 2) of the Kapiti-Manawatu long-term SSE (2021–2023), the highest frequency of seismic events in the KMR region reached 841 events per month during Stage 1 and 1091 events per month during Stage 2, significantly higher than the average monthly seismic frequency of 667 events per month from 2021 to 2023. Notably, one month prior to

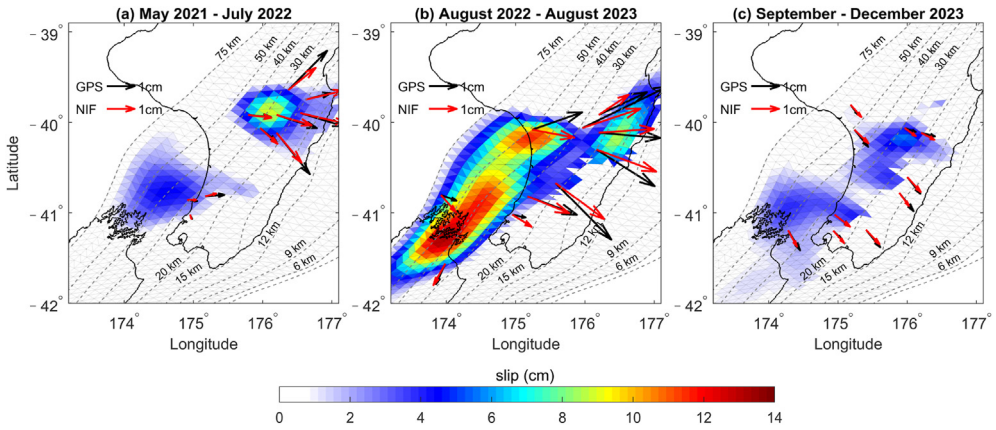

Fig. 7. Cumulative slip and surface displacement of Kapiti-Manawatu long-term SSE in three stages.

Table 1
Statistics of Kapiti-Manawatu long-term SSE from 2021 to 2023.

Kapiti-Manawatu long-term SSE	Stage 1	Stage 2	Stage 3
Duration	2021.05–2022.07	2022.08–2023.08	2023.09–2023.12
Months	15 months	13 months	4 months
Maximum monthly slip rate in Kapiti (cm/month)	2.03	3.43	2.01
Maximum monthly slip rate in Manawatu (cm/month)	4.26	4.01	4.40
Cumulative slip in Kapiti (cm)	4.47	13.21	3.77
Cumulative slip in Manawatu (cm)	8.94	11.55	5.51
Maximum GNSS horizontal displacement (cm)	1.77	3.31	0.73

the maximum slip rate in the Manawatu region, there is a significant increase in seismic activity.

In Table 2, the correlation between the monthly slip rates and the number of seismic events over the 36 months from 2021 to 2023 (as shown in Fig. 8(b)) is calculated. According to the correlation coefficient (usually above 0.7 is strong, 0.4 to 0.7 is medium, and below 0.4 is low), the correlation coefficient between the monthly slip rates in Manawatu and seismic events in KMR with a time delay of 1 month for seismic events was 0.59 (with a probability of 99.98 %), indicating a strong relationship between seismic activity in the KMR region and the slow slip in Manawatu, whereas there is no significant relationship with the slow slip in Kapiti. Furthermore, it is inferred that seismic activity in the KMR region likely contributed to the acceleration of slow slip in Manawatu.

4. Discussion

The Hikurangi subduction zone exhibits spatial migration in long-term SSEs from 2021 to 2023, with a gradual northeastward shift from Kapiti to Manawatu during the two complete cycles of spatial migration, consistent with historical long-term SSEs in the area [28]. Similarly, an along-strike migration pattern of SSEs is observed in the Nankai Subduction Zone in Japan from 1996 to 2017 [6]. This sequence of SSEs spanned four stages, migrating approximately 300 km from southern Hyuga-nada to western Shikoku, with a recurrence interval of about six years. These observations suggest that long-term SSEs are prone to significant spatial migration. The GNSS network, as a crucial tool for monitoring SSEs in subduction zones, offers high temporal resolution but is restricted in spatial resolution due to the limited density of GNSS station distribution. In contrast, Interferometric Synthetic Aperture Radar (InSAR) provides higher spatial resolution but limited temporal coverage, and it can only detect deformation in the radar line-of-sight direction [48]. Therefore, future research could employ an inversion of joint GNSS and InSAR data to reconstruct the evolution of long-term SSEs with high temporal and spatial resolution.

Moreover, there is a notable connection between the Kapiti-Manawatu long-term SSE and regional seismic activity from 2021 to 2023. Specifically, the slip rate in Manawatu is closely related to the number of seismic events in the Kapiti-Manawatu region. Remarkably, a significant increase in seismic frequency is observed one month before the slip rate in Manawatu reached its maximum. Furthermore, strong correlations are observed from 2019 to 2022 between short-term SSEs and seismic activity in the Hikurangi subduction zone, New Zealand, with a noticeable increase in seismic frequency during SSE occurrences [37,44,45]. Other studies also indicate a strong correlation between SSEs and seismic activity. For instance, prior to the Papanoya earthquake in Mexico, a long-term SSE began migrating towards the earthquake rupture zone until the earthquake occurred [12]. In 2014 and 2018, two long-term SSEs, each lasting approximately five months, are observed in the Hellenic Subduction Zone in Greece, accompanied by a significant increase in seismic activity [36]. Although numerous studies have indicated a correlation between SSEs and seismic activity, the underlying mechanisms of this relationship remain to be further studied.

Regarding the mechanism of triggering SSEs, stress perturbations induced by earthquakes are considered a key factor, influencing both their periodicity and slip rate. For example, the stress changes induced by the 2016 M_W7.8 Kaikōura earthquake in New Zealand triggered both shallow short-term slow slip in the northern part of the Hikurangi subduction zone and deep long-term slow slip in the southern part [25]. Similarly, the stress changes caused by the 2016 M_W7.6 Kumamoto earthquake in Japan alter the recurrence interval of the Bungo Channel long-term slow slip from 5 to 6 years prior to the earthquake to 7 years after the event [5]. By calculating Coulomb stress changes in the subduction zone, Wallace et al. hypothesizes that the 2010 Manawatu long-term slow slip may have activated the 2011

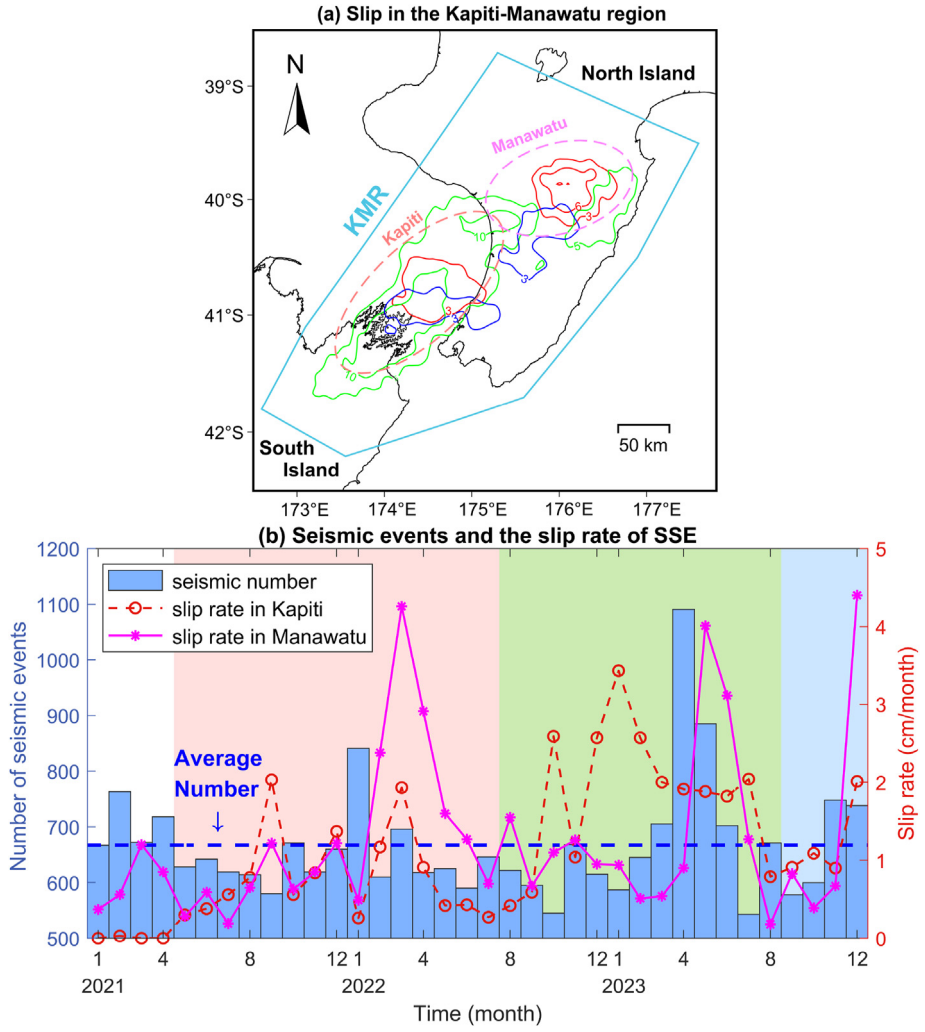

Fig. 8. Seismic activity and long-term SSE (2021–2023) slip rates in the Kapiti-Manawatu regions (KMR). (a) The KMR is delineated with a light blue thick solid line. The cumulative slips for the three phases of the Kapiti-Manawatu long-term SSE (2021–2023), namely Stage 1, Stage 2, and Stage 3, exceeding 3 cm, 5 cm, and 3 cm, respectively, are represented by red, green, and blue contour lines. (b) The number of seismic events occurring within the KMR (2021–2023) is statistically analyzed in relation to the monthly maximum slip rate in the Kapiti and Manawatu regions.

Table 2
Correlation analysis between monthly slip rates and the number of seismic events.

Correlation	Correlation coefficient					
Time delay of seismic events (Months)	−2	−1	0	1	2	3
Monthly slip rates in Kapiti and seismic events in KMR	0.26	0.22	−0.02	0.11	0.10	−0.10
Monthly slip rates in Manawatu and seismic events in KMR	−0.31	−0.13	0.18	0.59	0.36	−0.02

short-term slow slip on the East Coast [26]. Additionally, swarms of earthquakes occurring before SSEs suggest a fluid-related mechanism between the two phenomena [14]. For example, Heise et al. used magnetotelluric data to confirm the presence of fluids at the Hikurangi subduction interface [49], indicating a process of fluid migration along the subduction interface. Observations of fluid migration within the subducting plate before and after SSEs in the circum-Pacific subduction zones suggest that the accumulation and expulsion of fluids within the plate can trigger both seismic activity and SSEs. This rheological mechanism offers a plausible explanation for the link between SSEs and earthquake generation in subduction zones [4,22,23,50]. Existing research highlights various cases of mutual triggering between seismic activity and SSEs, with the timing and triggering mechanisms differing across regions, warranting further investigation.

5. Conclusions

Using displacement data from 53 continuously operating GNSS reference stations in the Kapiti-Manawatu region from 2019 to 2023, the long-term slow slip signals from 2021 to 2023 are extracted after removing tectonic movements and seasonal variations. The NIF method is then employed to mitigate the effects of common-mode error, reference oscillation, and random noise. A 3D fault grid model is constructed, and the fault Green's function is calculated to invert and obtain the spatiotemporal distribution of long-term slow slip at the central and southern edges of the

Hikurangi subduction zone in New Zealand. Finally, the relationship between the Kapiti-Manawatu long-term SSE and regional seismic activity is analyzed, leading to the following conclusions:

(1) From 2021 to 2023, the Kapiti-Manawatu long-term SSE exhibits spatial migration characteristics, with slip alternating between the Kapiti and Manawatu areas, along with intermittent stages of acceleration and deceleration. Accordingly, three stages can be approximately delineated: Stage 1 (May 2021 to July 2022), Stage 2 (August 2022 to August 2023), and Stage 3 (September 2023 to December 2023). Stage 3, with no subsequent deceleration observed at the end, is likely to continue into 2024. During the three stages, Manawatu experiences three instances of acceleration with maximum monthly slip rates exceeding 4 cm/month, while Kapiti experiences three instances of acceleration with maximum monthly slip rates ranging between 2 and 3.5 cm/month, indicating that the slip rate at Manawatu is significantly higher than that at Kapiti.
(2) The maximum cumulative slips in the Kapiti/Manawatu regions during the three stages are 4.47/8.94, 13.21/11.55, and 3.77/5.51 cm, respectively, with the corresponding maximum surface displacements monitored by GNSS being 1.77, 3.31, and 0.73 cm, respectively. Notably, during the two complete cycles of spatial migration and acceleration-deceleration (Stage 1 and Stage 2), both the cumulative slip and surface displacement during Stage 2 are greater than those observed in Stage 1.
(3) The highest seismic frequency in the KMR region reached 841 events per month during Stage 1 and 1091 events per month during Stage 2, significantly higher than the average monthly seismic frequency of 667 events per month from 2021 to 2023. The correlation coefficient between the monthly slip rates in Manawatu and seismic events in KMR with a time delay of 1 month is 0.59, indicating a moderate correlation between seismic activity in the KMR region and the slow slip in Manawatu. This temporal correlation suggests that seismic activity in the KMR region likely contributed to the acceleration of slow slip in Manawatu. In contrast, there is no significant relationship between seismic activity in the KMR region and the slow slip at Kapiti.

CRediT authorship contribution statement

Li Yan: Writing – review & editing, Writing – original draft, Visualization, Validation, Supervision, Software, Resources, Project administration, Methodology, Investigation, Funding acquisition, Formal analysis, Data curation, Conceptualization. **Yanling Sun:** Visualization, Validation, Software, Investigation, Formal analysis, Data curation. **Meng Li:** Writing – review & editing, Validation, Supervision, Software, Investigation, Funding acquisition, Conceptualization. **Ahmed El-Mowafy:** Writing – review & editing, Validation, Supervision, Investigation, Formal analysis. **Tieding Lu:** Writing – review & editing, Validation, Supervision, Investigation, Funding acquisition.

Declaration of competing interest

The authors declare that they have no known competing financial interests or personal relationships that could have appeared to influence the work reported in this paper.

Acknowledgments

We acknowledge the New Zealand GeoNet programme and its sponsors EQC, GNS Science, LINZ, NEMA and MBIE for providing data used in this study.

This research was funded by the National Natural Science Foundation of China (41704031, 42374040); the Natural Science Foundation of Jiangxi Science and Technology Department (20232BAB203073); the Key Laboratory of Mine Environmental Monitoring and Improving around Poyang Lake, Ministry of Natural Resources (MEMI-2021-2022-29).

Appendix A. Supplementary data

Supplementary data to this article can be found online at https://doi.org/10.1016/j.geog.2024.12.001.

References

[1] S.Y. Schwartz, J.M. Rokosky, Slow slip events and seismic tremor at circum-pacific subduction zones, Rev. Geophys. 45 (2007) 8755–1209, https://doi.org/10.1029/2006RG000208.
[2] A. Ducellier, K.C. Creager, D.A. Schmidt, Detection of slow slip events using wavelet analysis of GNSS recordings, Bull. Seismol. Soc. Am. 112 (2022) 2408–2424, https://doi.org/10.1785/0120210289.
[3] S. Song, M. Hao, Y. Li, Q. Wang, Extraction of transient signal from GPS position time series by employing ICA, Geodesy Geodyn. 14 (2023) 597–604, https://doi.org/10.1016/j.geog.2023.04.004.
[4] K. Obara, A. Kato, Connecting slow earthquakes to huge earthquakes, Science 353 (2016) 253–257, https://doi.org/10.1126/science.aaf1512.
[5] S. Ozawa, R. Kawabata, K. Kokado, H. Yarai, Long-term slow slip events along the Nankai trough delayed by the 2016 Kumamoto earthquake, Japan, Earth Planets Space 72 (2020) 61, https://doi.org/10.1186/s40623-020-01189-z.
[6] T. Ryota, U. Naoki, O. Kazushige, Along-strike variation and migration of long-term slow slip events in the western Nankai subduction zone, Japan, J. Geophys. Res. Solid Earth 124 (2019) 3853–3880, https://doi.org/10.1029/2018jb016738.
[7] M. Li, L. Yan, Z. Jiang, G. Xiao, Insights into spatio-temporal slow slip events offshore the Boso Peninsula in central Japan during 2011–2019 using GPS data, Geodesy Geodyna. 13 (2022) 554–563, https://doi.org/10.1016/j.geog.2022.03.006.
[8] C.P. Nuyen, D.A. Schmidt, Filling the gap in Cascadia: the emergence of low-amplitude long-term slow slip, Geochem. Geophys. Geosys. 22 (2021) e2020GC009477, https://doi.org/10.1029/2020gc009477.
[9] N.M. Bartlow, A long-term view of episodic tremor and slip in Cascadia, Geophys. Res. Lett. 47 (2020) e2019GL085303, https://doi.org/10.1029/2019gl085303.
[10] V. Kostoglodov, S.K. Singh, J.A. Santiago, S.I. Franco, K.M. Larson, et al., A large silent earthquake in the Guerrero seismic gap, Mexico, Geophys. Res. Lett. 30 (2003) 1807, https://doi.org/10.1029/2003gl017219.
[11] M. Radiguet, F. Cotton, M. Vergnolle, M. Campillo, B. Valette, et al., Spatial and temporal evolution of a long term slow slip event: the 2006 Guerrero Slow Slip Event, Geophys. J. Int. 184 (2011) 816–828, https://doi.org/10.1111/j.1365-246X.2010.04866.x.
[12] M. Radiguet, H. Perfettini, N. Cotte, A. Gualandi, B. Valette, et al., Triggering of the 2014 Mw7.3 Papanoa earthquake by a slow slip event in Guerrero, Mexico, Nat. Geosci. 9 (2016) 829–833, https://doi.org/10.1038/ngeo2817.
[13] L. Zhang, D. Huang, C.K. Shum, R. Guo, The 2019 East Coast slow slip event, New Zealand: spatiotemporal evolution and associated seismicity, Mar. Geodesy (2022) 195–215, https://doi.org/10.1080/01490419.2022.2141931.
[14] T. Nishikawa, T. Nishimura, Y. Okada, Earthquake swarm detection along the Hikurangi Trench, New Zealand: insights into the relationship between seismicity and slow slip events, J. Geophys. Res. Solid Earth 126 (2021) e2020JB020618, https://doi.org/10.1029/2020jb020618.
[15] E.K. Todd, S.Y. Schwartz, Tectonic tremor along the northern Hikurangi margin, New Zealand, between 2010 and 2015, J. Geophys. Res. Solid Earth 121 (2016) 8706–8719, https://doi.org/10.1002/2016JB013480.
[16] W. Wang, M.K. Savage, A. Yates, H.J. Zal, S. Webb, et al., Temporal velocity variations in the northern Hikurangi margin and the relation to slow slip, Earth Planet Sci. Lett. 584 (2022) 117443, https://doi.org/10.1016/j.epsl.2022.117443.
[17] P.M. Barnes, L.M. Wallace, D.M. Saffer, R.E. Bell, M.B. Underwood, et al., Slow slip source characterized by lithological and geometric heterogeneity, Sci. Adv. 6 (2020) eaay3314, https://doi.org/10.1126/sciadv.aay3314.
[18] L.M. Wallace, Slow slip events in New Zealand, Annu. Rev. Earth Planet Sci. 48 (2020) 175–203, https://doi.org/10.1146/annurev-earth-071719-055104.
[19] A. Perez-Silva, Y. Kaneko, M. Savage, L. Wallace, D. Li, et al., Segmentation of shallow slow slip events at the Hikurangi subduction zone explained by

along-strike changes in fault geometry and plate convergence rates, J. Geophys. Res. Solid Earth 127 (2022) e2021JB022913, https://doi.org/10.1029/2021JB022913.
[20] K. Woods, S.C. Webb, L.M. Wallace, Y. Ito, C. Collins, et al., Using seafloor geodesy to detect vertical deformation at the Hikurangi subduction zone: insights from self-calibrating pressure sensors and ocean general circulation models, J. Geophys. Res. Solid Earth 127 (2022) e2022JB023989, https://doi.org/10.1029/2022jb023989.
[21] R. Yohler, N. Bartlow, L.M. Wallace, C. Williams, Time-dependent behavior of a near-trench slow-slip event at the Hikurangi subduction zone, Geochem. Geophys. Geosys. 20 (2019) 4292–4304, https://doi.org/10.1029/2019GC008229.
[22] E. Warren-Smith, S. Schwartz, S. Webb, B. Fry, L. Wallace, et al., Episodic stress and fluid pressure cycling in subducting oceanic crust during slow slip, Nat. Geosci. 12 (2019) 475–481, https://doi.org/10.1038/s41561-019-0367-x.
[23] L.M. Wallace, D. Eberhart-Phillips, Newly observed, deep slow slip events at the central Hikurangi margin, New Zealand: implications for downdip variability of slow slip and tremor, and relationship to seismic structure, Geophys. Res. Lett. 40 (2013) 5393–5398, https://doi.org/10.1002/2013gl057682.
[24] K. Woods, Investigation of Hikurangi subduction zone slow slip events using onshore and offshore geodetic data, Victoria University of Wellington, Wellington, New Zealand, 2022, https://doi.org/10.26686/wgtn.21300411.
[25] L.M. Wallace, S. Hreinsdóttir, S. Ellis, I. Hamling, E. D'Anastasio, et al., Triggered slow slip and afterslip on the southern Hikurangi subduction zone following the Kaikōura earthquake, Geophys. Res. Lett. 45 (2018) 4710–4718, https://doi.org/10.1002/2018gl077385.
[26] L.M. Wallace, J. Beavan, S. Bannister, C. Williams, Simultaneous long-term and short-term slow slip events at the Hikurangi subduction margin, New Zealand: implications for processes that control slow slip event occurrence, duration, and migration, J. Geophys. Res. Solid Earth 117 (2012) B11402, https://doi.org/10.1029/2012jb009489.
[27] L.M. Wallace, N. Bartlow, I. Hamling, B. Fry, Quake clamps down on slow slip, Geophys. Res. Lett. 41 (2014) 8840–8846, https://doi.org/10.1002/2014GL062367.
[28] L.M. Wallace, J. Beavan, Diverse slow slip behavior at the Hikurangi subduction margin, New Zealand, J. Geophys. Res. 115 (2010) B12402, https://doi.org/10.1029/2010jb007717.
[29] H. Hirose, T. Matsushima, T. Tabei, T. Nishimura, Long-term slow slip events with and without tremor activation in the Bungo Channel and Hyuganada, southwest Japan, Earth Planets Space 75 (2023) 75–77, https://doi.org/10.1186/s40623-023-01833-4.
[30] L. Yan, Y. Sun, M. Li, A. El-Mowafy, L. Ma, Slow slip events associated with seismic activity in the Hikurangi subduction zone, New Zealand, from 2019 to 2022, Rem. Sens. 15 (2023) 4767, https://doi.org/10.3390/rs15194767.
[31] A. Koulali, S. McClusky, L. Wallace, S. Allgeyer, P. Tregoning, et al., Slow slip events and the 2016 Te Araroa Mw7.1 earthquake interaction: Northern Hikurangi subduction, New Zealand, Geophys. Res. Lett. 44 (2017) 8336–8344, https://doi.org/10.1002/2017gl074776.
[32] N.M. Bartlow, L.M. Wallace, R.J. Beavan, S. Bannister, P. Segall, Time-dependent modeling of slow slip events and associated seismicity and tremor at the Hikurangi subduction zone, New Zealand, J. Geophys. Res. Solid Earth 119 (2014) 734–753, https://doi.org/10.1002/2013jb010609.
[33] L.M. Wallace, J. Beavan, A large slow slip event on the central Hikurangi subduction interface beneath the Manawatu region, North Island, New Zealand, Geophys. Res. Lett. 33 (2006) L11301, https://doi.org/10.1029/2006gl026009.
[34] P. Romanet, S. Ide, Ambient tectonic tremors in Manawatu, Cape Turnagain, Marlborough, and Puysegur, New Zealand, Earth Planets Space 71 (2019) 59, https://doi.org/10.1186/s40623-019-1039-1.
[35] I.J. Hamling, L.M. Wallace, Silent triggering: aseismic crustal faulting induced by a subduction slow slip event, Earth Planet Sci. Lett. 421 (2015) 13–19, https://doi.org/10.1016/j.epsl.2015.03.046.
[36] V. Saltogianni, V. Mouslopoulou, A. Dielforder, G.M. Bocchini, J. Bedford, et al., Slow slip triggers the 2018 Mw 6.9 Zakynthos Earthquake within the weakly locked Hellenic subduction system, Greece, Geochem. Geophys. Geosys. 22 (2021) e2021GC010090, https://doi.org/10.1029/2021gc010090.
[37] P. Segall, M. Matthews, Time dependent inversion of geodetic data, J. Geophys. Res. Solid Earth 102 (1997) 22391–22409, https://doi.org/10.1029/97jb01795.
[38] S.i. Miyazaki, P. Segall, J.J. McGuire, T. Kato, Y. Hatanaka, Spatial and temporal evolution of stress and slip rate during the 2000 Tokai slow earthquake, J. Geophys. Res. Solid Earth 111 (2006) 148–227, https://doi.org/10.1029/2004jb003426.
[39] N.M. Bartlow, S.i. Miyazaki, A.M. Bradley, P. Segall, Space-time correlation of slip and tremor during the 2009 Cascadia slow slip event, Geophys. Res. Lett. 38 (2011) L18309, https://doi.org/10.1029/2011gl048714.
[40] Y. Jiang, Z. Liu, E.E. Davis, S.Y. Schwartz, T.H. Dixon, et al., Strain release at the trench during shallow slow slip: the example of Nicoya Peninsula, Costa Rica, Geophys. Res. Lett. 44 (2017) 4846–4854, https://doi.org/10.1002/2017gl072803.
[41] L. Yan, Z.D. Luo, A.P. Zhao, M. Li, D.D. Yan, NIF inversion and spatiotemporal analysis of GPS monitoring slow slip events, Geomatics Inf. Sci. Wuhan Univ. (2022) 1–13, https://doi.org/10.13203/j.whugis20220103.
[42] B. Chow, Y. Kaneko, J. Townend, Evidence for deeply subducted lower-plate seamounts at the Hikurangi Subduction Margin: implications for seismic and aseismic behavior, J. Geophys. Res. Solid Earth 127 (2022) e2021JB022866, https://doi.org/10.1029/2021JB022865.
[43] C.A. Williams, D. Eberhart-Phillips, S. Bannister, D.H.N. Barker, S. Henrys, et al., Revised interface geometry for the Hikurangi subduction zone, New Zealand, Seismol Res. Lett. 84 (2013) 1066–1073, https://doi.org/10.1785/0220130035.
[44] P. Segall, R. Bürgmann, M. Matthews, Time-dependent triggered afterslip following the 1989 Loma Prieta earthquake, J. Geophys. Res. Solid Earth 105 (2000) 5615–5634, https://doi.org/10.1029/1999jb900352.
[45] S.i. Miyazaki, J.J. McGuire, P. Segall, A transient subduction zone slip episode in southwest Japan observed by the nationwide GPS array, J. Geophys. Res. Solid Earth 108 (2003) 2087, https://doi.org/10.1029/2001jb000456.
[46] K. Ansari, J. Walo, A.V.H. Simanjuntak, K. Wezka, Evaluation of recent tectonic movement in northeast Japan by using long-term GNSS and tide gauge measurements, J. Struct. Geol. 188 (2024), https://doi.org/10.1016/j.jsg.2024.105258.
[47] L.M. Wallace, Y. Kaneko, S. Hreinsdóttir, I. Hamling, Z. Peng, et al., Large-scale dynamic triggering of shallow slow slip enhanced by overlying sedimentary wedge, Nat. Geosci. 10 (2017) 765–770.
[48] D.P.S. Bekaert, P. Segall, T.J. Wright, A.J. Hooper, A Network Inversion Filter combining GNSS and InSAR for tectonic slip modeling, J. Geophys. Res. Solid Earth 121 (2016) 2069–2086, https://doi.org/10.1002/2015jb012638.
[49] W. Heise, T.G. Caldwell, S. Bannister, E.A. Bertrand, Y. Ogawa, et al., Mapping subduction interface coupling using magnetotellurics: Hikurangi margin, New Zealand, Geophys. Res. Lett. 44 (2017) 9261–9266, https://doi.org/10.1002/2017gl074641.
[50] S.K. Chen, Y.M. Wu, Y.C. Chan, Episodic slow slip events and overlying plate seismicity at the southernmost Ryukyu Trench, Geophys. Res. Lett. 45 (2018) 10369–10377, https://doi.org/10.1029/2018GL079740.

Dr. Li Yan is a lecturer at the Department of Surveying Engineering, East China University of Technology, and a visiting research associate at Curtin University's School of Earth and Planetary Sciences. She earned her Ph.D. in Geodesy and Surveying Engineering from Southwest Jiaotong University in 2017. Her research focuses on satellite navigation positioning theory and algorithms, and crustal dynamics.